Human Pathology (2019) **89**, 33–39

ELSEVIER

Human PATHOLOGY

www.elsevier.com/locate/humpath

Original contribution

Activating *KRAS* mutations in arteriovenous malformations of the brain: frequency and clinicopathologic correlation☆,☆☆

David S. Priemer MD, Alexander O. Vortmeyer MD, Shaobo Zhang MD, Hsim Yee Chang MLS(ASCP), Kendra L. Curless MLS(ASCP), Liang Cheng MD*

Department of Pathology and Laboratory Medicine, Indiana University School of Medicine, Indianapolis, IN, 46202

Received 3 October 2018; revised 8 April 2019; accepted 11 April 2019

Keywords:
Brain;
Arteriovenous malformation;
Hemangioma;
KRAS;
Molecular genetics;
Differential diagnosis

Summary Arteriovenous malformations (AVM) of the brain are considered congenital. Most AVMs are presumably sporadic; however, rare familial cases occur and they may be observed in certain genetic disorders. We sought to determine the frequency of *KRAS* mutations and their association with clinicopathologic characteristics. We searched our neuropathology database from 2014–2017 for resected AVMs of the brain or dura mater. Twenty-one AVMs were tested (12 females, 9 males; average age: 32 years). *KRAS* mutations were found in 6/21 cases (28.5%). Five mutations were p.G12 V, and one p.G12C. The *KRAS*-mutant group contained 4 females and 2 males, with an average age of 28 years, compared to 34 years in the non-mutant group (P = .54). The average AVM size in the *KRAS*-mutant group was 3.9 cm, compared to 3.1 cm in the non-mutant group (P = .52). There were no histologic differences between *KRAS*-mutant and non-mutant cases. In summary, *KRAS* mutations occur in almost one-third of brain AVMs. *KRAS* p.G12 V was the most common mutation identified. We also demonstrate the first reported instance of a *KRAS* p.G12C mutation in a brain AVM. The mean age of patients with *KRAS*-mutant AVMs was lower than the non-mutant group, and the mean size larger. Histologic characteristics were equally distributed between *KRAS*-mutant and non-mutant groups.

1. Introduction

Brain arteriovenous malformations (AVM) are fistulous aggregations of arterial and venous vessels, are considered to be congenital, and may present across a large age range [1]. They have an incidence of up to approximately 2 per 100 000 person-years [2], and are responsible for approximately 4% of intracerebral hemorrhages, including up to one-third of intracerebral hemorrhages in young adults [3]. Most brain AVMs are presumably sporadic, but rare familial cases have been reported [4] and they may be observed in genetic disorders such as hereditary hemorrhagic telangiectasia [5], capillary malformation-arteriovenous malformation syndrome [6], and Wyburn-Mason syndrome [7].

Recently, Nikolaev et al reported *KRAS* mutations in tissue from 45/72 brain AVMs (62.5%), but none within 21 paired blood samples [8]. In the same study, *KRAS* mutations were detected in endothelial cells from human brain AVMs in vitro and it was noted that mutant *KRAS* expression

☆ Conflict of interest: None.
☆☆ Funding: None.
* Corresponding author at: Molecular Pathology Laboratory, Department of Pathology and Laboratory Medicine, Indiana University School of Medicine, 350 West 11th Street, IUHPL Room 4010, Indianapolis, IN 46202, USA.
E-mail address: liang_cheng@yahoo.com (L. Cheng).

https://doi.org/10.1016/j.humpath.2019.04.004
0046-8177/

initiated increased ERK activity that was counteracted by inhibition of mitogen-activated protein kinase (MAPK)–ERK signaling. In addition, based on immunohistochemistry of 25 AVMs, Nikolaev et al concluded that activation of the MAPK–ERK pathway is a defining molecular signature of AVMS. The initiating events for AVMs without RAS mutations are uncertain; however, the pathogenetic mechanisms resulting from RAS-initiated activation of the MAPK–ERK pathway are mediated by angiogenic genes (eg, *VEGF A/C*) and proteins in the notch signaling pathway [9-12]. In this study, we postulated that these mechanisms may result in potentially distinguishable clinical and/or histologic features between *KRAS*-mutant and non-mutant AVMs.

2. Materials and methods

2.1. Cases

A search of our neuropathology archives for intracranial AVMs was performed from 2014–2017. Hematoxylin and eosin (H&E)–stained and Verhoeff-van Gieson–stained slides were reviewed to confirm the diagnosis according to published texts [13,14]. Slides were also examined to tissue adequacy and viability for molecular testing. Cases were excluded from molecular testing if the tissue amount was insufficient or if the tissue was felt to be extensively damaged by artifact (eg, cautery).

Reviews of electronic clinical records were performed for patient age, gender, presenting symptoms, and past medical history (with particular reference to history of additional intracranial or extracranial vascular lesions). Imaging studies were reviewed to document the size and location of the AVM nidus. Family histories were also reviewed, particularly for history of brain AVMs, other vascular lesions, or stroke.

After identification of *KRAS*-mutant and non-mutant cases, H&E-stained and Verhoeff-van Gieson-stained slides were reexamined for differing histology between groups. Immunohistochemical stains for Ki-67 (Clone MIB-1; Dako, Santa Clara, CA) were also performed. The principle features considered in this examination included general diagnostic architectural characteristics, evidence of proliferative activity (mitoses, Ki-67 labeling in endothelial cells and vascular smooth muscle cells), and proportion of vascular channels with and without elastic laminae (either partial or complete circumferential staining). This research was approved by the Institutional Review Board.

2.2. KRAS mutational analysis

Formalin-fixed, paraffin-embedded (FFPE) tissue blocks were retrieved from each included case. *KRAS* mutation analysis was performed in a Clinical Laboratory Improvements and Amendments (CLIA) certified molecular pathology laboratory. DNA extraction from each block was performed using the Qiagen QIAamp DNA FFPE Tissue Kit (Qiagen, Valencia, CA). DNA concentration was determined using the NanoDrop Spectrophotometer and adjusted to approximately 10 ng/μl in ddH2O. Polymerase chain reaction (PCR) testing was performed according to the recommended procedure using the Qiagen therascreen *KRAS* RGQ PCR Kit on the Qiagen Rotor-Gene Q MDx instrument. The therascreen *KRAS* RGQ PCR Kit provides eight separate PCR amplification reactions: seven mutation-specific reactions in codons 12 and 13 of exon 2 of the *KRAS* oncogene, and a

Table Arteriovenous malformation of the brain: individual case data

Case	Age	Sex	Presentation	AVM Location	AVM Side	AVM Size (cm)	*KRAS* status
1	24	Female	Seizure	Frontal lobe	Left	4.9	Wild-type
2	27	Female	Hemorrhage	Frontal lobe	Left	3.0	Wild-type
3	38	Male	Hemorrhage	Temporal lobe	Left	5.7	Wild-type
4	9	Female	Hemorrhage	Temporal lobe	Left	3.5	G12 V
5	65	Male	Hemorrhage	Parietal lobe	Right	9.0	G12 V
6	54	Female	Hemorrhage	Temporal lobe	Right	3.5	Wild-type
7	30	Female	Headache	Frontal lobe	Left	3.0	G12 V
8	57	Male	Hemorrhage	Frontal lobe	Left	2.5	Wild-type
9	34	Male	Incidental	Parietal lobe	Right	1.7	Wild-type
10	13	Female	Hemorrhage	Frontal lobe	Right	4.1	G12 V
11	32	Female	Hemorrhage	Occipital lobe	Left	2.0	G12C
12	18	Male	Headache	Parietal lobe	Right	1.7	G12 V
13	55	Female	Seizure	Temporal lobe	Right	2.3	Wild-type
14	34	Male	Headache	Frontal lobe	Left	2.5	Wild-type
15	20	Female	Hemorrhage	Cerebellum	Midline	3.0	Wild-type
16	16	Female	Headache	Parietal lobe	Left	4.4	Wild-type
17	18	Male	Hemorrhage	Occipital lobe	Right	2.6	Wild-type
18	40	Male	Seizure	Frontal lobe	Left	2.5	Wild-type
19	11	Female	Headache	Frontal lobe	Left	2.0	Wild-type
20	40	Female	Seizure	Parietal lobe	Left	3.0	Wild-type
21	36	Male	Tinnitus	Dura	Midline	Not listed	Wild-type

wild-type control in exon 4. Analysis of crossing thresholds and mutation calls for each PCR amplification reaction were performed by the Rotor-Gene Q therascreen *KRAS* Assay Package once runs were completed.

2.3. Statistical analysis

Student *t* tests were performed to assess for significance between patient age, gender, and AVM sizes in *KRAS*-mutant and non-mutant groups. Fisher's exact test was used to compare categorical data for clinicopathologic characteristics between *KRAS* mutated and non-mutant groups. Statistical significance was defined as $P < .05$ and all *P* values were 2-tailed.

3. Results

Twenty-one AVM resections diagnosed by our neuropathology service from 2014–2017 were determined to be viable and sufficient for molecular testing. Slide review confirmed the AVM diagnosis in all cases. This 21-case cohort included material from 12 females and 9 males. The average patient age was 32 years (median: 32 years; range: 9–65 years). Table T1 contains a summary of data from each case.

Clinical records revealed that only one patient, an 11-year-old girl with a left frontal lobe AVM, had a history of an additional vascular malformation that was within the parotid gland. No patients had multiple intracranial AVMs. No patients had a family history of intracranial AVMs or extracranial vascular

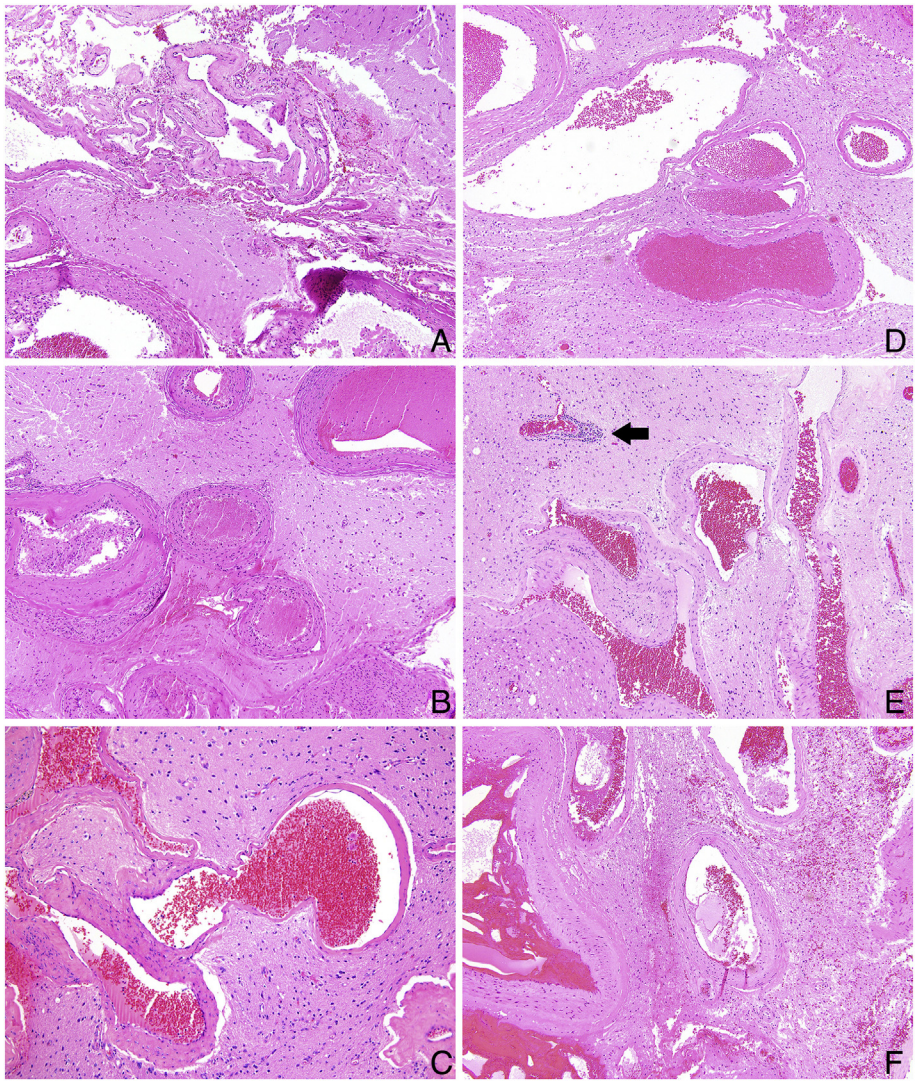

Fig. 1 Photomicrographs of brain arteriovenous malformations (AVMs), 100x magnification. A-C, Non-mutant AVMs. D-F, *KRAS*-mutant AVMs. All AVMs displayed the conventional histology of mixed arterial and venous channels, and 'arterialized veins' embedded in gliotic brain parenchyma, and were occasionally noted with hemorrhage (B and F) and inflammatory infiltrates (arrow) (E). *KRAS*-mutant and non-mutant AVMS were not distinguishable histologically.

lesions. Only one patient had a family history of stroke, but the cause was not indicated. The most common presenting symptom was hemorrhage (10 cases, 48%), followed by headache (5 cases, 24%), seizure (4 cases, 19%), and tinnitus (1 case, 5%). In one case, the AVM was incidentally discovered. The AVM locations were intraparenchymal within the brain in 20 cases, and dural-based in 1 case. When intraparenchymal, most AVMs were intracerebral (frontal lobe: 8 cases, parietal lobe: 5 cases, temporal lobe: 4 cases, occipital lobe: 2 cases). One case was cerebellar. AVM size was reported in 20/21 cases. The average AVM size was 3.3 cm (median: 3 cm, range: 1.7-9.0 cm).

KRAS mutation analysis revealed mutations in 6/21 cases (28.5%). Five of the 6 mutated cases involved p.G12 V mutations, and 1 involved a p.G12C mutation. The *KRAS*-mutant group contained 4 females and 2 males, and the average patient age was 28 years (median: 24 years, range: 9–65 years). Presenting symptoms for the AVMs in the *KRAS*-mutant group included 4 cases with hemorrhage and 2 with headaches. All 6 of the *KRAS*-mutant cases were intracerebral (frontal lobe: 2 cases, temporal lobe: 2 cases, parietal lobe: 1 case, occipital lobe: 1 case). The average AVM size in the *KRAS*-mutant group was 3.9 cm. The non-mutant group contained 8 females and 7 males, and the average age was 34 years (median: 34 years, range: 11–57 years).\.

Presenting symptoms for the AVMs in the non-mutant group included 6 cases with hemorrhage, 4 with seizures, 3

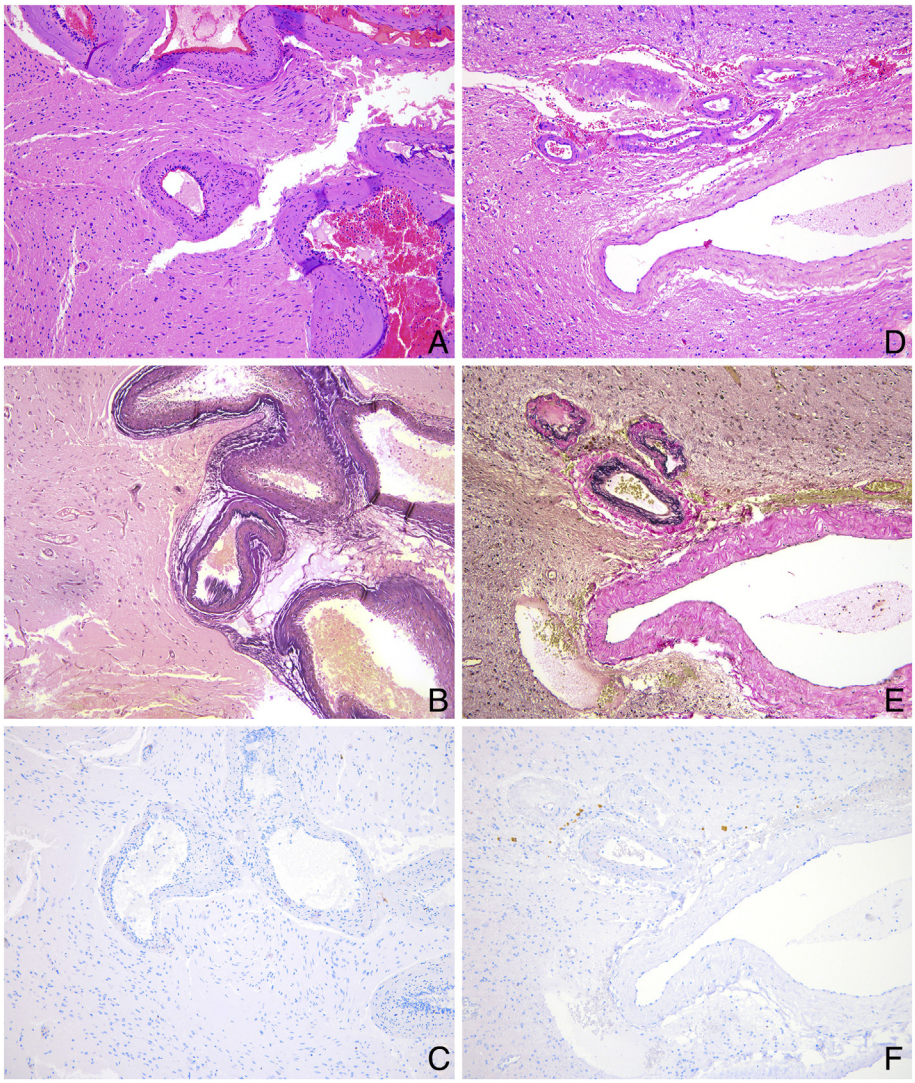

Fig. 2 Photomicrographs of brain arteriovenous malformations (AVMs), 100x magnification. A-C, Non-mutant AVM case. D-F, *KRAS*-mutant AVM case. Comparison of H&E Eosin ; (A and D), Verhoeff-van Gieson stains (B and E), and Ki-67 immunohistochemical stains (C and F). Regardless of mutation status, all AVMs displayed the conventional histology of mixed arterial and venous channels, and 'arterialized veins', evidenced further by discontinuities in the elastic lamina as demonstrated by Verhoeff-van Gieson staining. Also, both KRAS-mutant and non-mutant AVMs all similarly displayed little to no evidence of proliferative activity via Ki-67 immunohistochemical staining, with stains essentially being negative in all components of the lesions (proliferative index of <1%). The foci of brown discoloration in photomicrograph F are hemosiderin deposits.

with headaches, 1 with tinnitus, and 1 was incidentally discovered. The average AVM size in the non-mutant group was 3.1 cm (n = 14). There was no significant difference between *KRAS*-mutant and non-mutant groups regarding age (P = .546), AVM size (P = .522), or gender (P = .659). The patients with the aforementioned family history of stroke and personal history of a vascular malformation in the parotid gland were in the non-mutant group.

Examination of H&E-stained slides revealed similar diagnostic histologic features between *KRAS*-mutant and non-mutant groups (Fig. 1). Mitotic figures were not readily identified in either group. Examination of Verhoeff-van Gieson-stained slides revealed that the average ratio of AVM vessels containing completely or partially circumferential elastic laminae to those that do not was 0.42 overall (range, 0.25–0.75). The average ratio for *KRAS*-mutant AVMs was 0.46 (range, 0.25–0.75), compared to 0.41 (range, 0.25–0.67) in non-mutant AVMs. Ki-67 immunohistochemical stains performed on sections from each case revealed labeling that was <1% in all cases, whether *KRAS*-mutant or non-mutant, in both the endothelial cells and smooth muscle cells of the AVM vessels (Fig. 2).

4. Discussion

Brain AVMs are a common cause of intracranial hemorrhage. In addition to clinical presentations relating to hemorrhage, brain AVMs can also have presentations including seizures or headaches, while others (at least 15%) are asymptomatic [3]. Most AVMs are presumably sporadic, but there are rare familial cases and AVMs also occur in a number of congenital syndromes [4-7]. For example, there is a 4–13% prevalence of brain AVMs in patients with hereditary hemorrhagic telangiectasia [15,16]. Recently, activating *KRAS* mutations were noted in 62.5% of 72 brain AVMs, but in none of 21 paired blood samples [8]. The *KRAS* mutations reported, in order of frequency, were p.G12D, p.G12 V, and p.Q61H. In this study, we investigated *KRAS* mutations in brain AVMs and compared basic clinical and histologic information to assess for distinguishing features between *KRAS*-mutant and non-mutant AVMs.

Of 21 brain AVM cases in our cohort, 6 (28.5%) contained *KRAS* mutations by PCR. We thus demonstrate that a subset of brain AVMs contain *KRAS* mutations and confirm that *KRAS* mutations should be considered among possible mutations in AVMs that may represent key genetic drivers in their development. Other mutations reported in vascular malformations include somatic mutations in the RAS-MAPK pathway, which have been noted in brain AVMs, and mutations in the PI3K pathway [17-21]. Interestingly, *KRAS* is mostly implicated in tumorigenesis and cancer, where mutations promote unregulated activation of growth-promoting signal transduction pathways resulting in cell transformation and genomic instability [9-12]. The presence of *KRAS* mutations in brain AVMs thus raises the question of whether they may represent a neoplastic process rather than a malformative one. However, though activating *KRAS* mutations are usually affiliated with malignancy, brain AVMs are not known to have malignant potential. Also worth noting is that there may be different roles of *KRAS* mutations in the contexts of different disease processes. For example, endometriosis is essentially not associated with malignancy, but about one quarter of deep infiltrating endometriotic lesions have been reported to harbor driver mutations associated with cancer, including *KRAS* mutations [22]. Substantially more research is necessary in order to reach an understanding of cancer-associated driver mutations in the setting of benign, and even potentially non-neoplastic disease processes. *KRAS* mutations in brain AVMs may also have interesting implications with regard to therapy, as our knowledge of *RAS* oncogenes and potentially targetable, *RAS*-associated proteins and processes grows and therapies are put into clinical use [23,24].

The most common *KRAS* mutation in our cohort was p.G12 V, and no cases harbored a p.G12D mutation. This is in contrast to a previous report that detected p.G12D as the most common *KRAS* mutation in brain AVMs, followed by p.G12 V [8]. In one case, our study also detected a p.G12C mutation in a brain AVM, and this has not been previously reported. This finding is of interest considering that *KRAS* p.G12C mutations have been recently identified as potentially targetable in cancer therapy and p.G12C inhibitors are currently being investigated [25-28].

Clinical information in our cohort revealed no distinguishing features between *KRAS*-mutant and non-mutant groups. No patients had a history of multiple brain AVMs. Only one patient, a child with an AVM in the non-mutant group, had an additional vascular malformation outside of the brain. There were no documented family histories of intra- or extracranial vascular malformations. Presenting symptoms between the groups were similar, but none in the *KRAS*-mutant group presented with seizures. The average age in the *KRAS*-mutant group (28 years) was lower than the non-mutant group (34 years), but the oldest patient in the study was in the *KRAS*-mutant group, and the age difference was not statistically significant. The average AVM size was larger in the *KRAS*-mutant group (3.9 cm) than the non-mutant group (3.1 cm), but this also was not statistically significant. Additional studies with larger cohorts are necessary to definitively determine if there are substantive differences in patient age and AVM size between *KRAS*-mutant and non-mutant cases. Finally, conventional histology for brain AVMs was observed in all cases of our study and histologic characteristics, including proportions of elastin-containing vessels and evidence of proliferative activity, were equally distributed and similarly present in all brain AVMs regardless of *KRAS* status. Nikolaev et al reported that *KRAS* mutations in the endothelial cells of brain AVMs in vitro initiated activation of the MAPK–ERK pathway [8]. They also concluded immunohistochemically that MAPK–ERK activation is a defining molecular feature of brain AVMs, with or without initiation by a *KRAS* mutation. Initiating events for AVMs without RAS mutation are uncertain. The result of our histologic investigation between *KRAS*-mutant and non-mutant AVMs likely indicates that the

histology of brain AVMs is not specific to activating *KRAS* mutations. Instead, it may indicate that the histology of brain AVMs is a reflection of MAPK–ERK activation in general, regardless of the initiating event. This suggests that the presence of *KRAS* mutations within AVMs may be of little clinical or pathologic importance.

The frequency of *KRAS* mutations in brain AVMS noted in our study is lower than previously reported. There may be several reasons for this discrepancy. The first may be divergence in methodology. Our study implemented a therascreen *KRAS* RGQ PCR Kit, a FDA approved real-time PCR assay that detects 7 mutations in codons 12 and 13 of exon 2 of the *KRAS* gene. The estimated limit of detection (analytical sensitivity) of the *KRAS* assay in our laboratory is 1%. The original publication by Nikolaev et al used droplet digital PCR, and established a minimum of 0.5% fractional abundance for a positive sample [8]. Discrepancy may also be due to difference in materials. Our study utilized only FFPE for real-time PCR testing, while the previous study utilized both FFPE and fresh frozen tissues for genetic analysis [8]. However, a large analysis of DNA quality from FFPE tissues was published by Einaga et al [29], and the results showed that the DNA extracted from FFPE tissue was sufficient for sequencing based tests.

Tissue sampling may also have contributed to discrepancy: brain AVMs contain numerous cell types and, as previously reported, it is endothelial cells that contain *KRAS* mutations in brain AVMs [8]. It is possible that mutations were undetected in some cases owing to undersampling of endothelial cells relative to other AVM components. Finally, there may be some discrepancy as a result of a potential difference in our patient population. Further studies would be necessary to assess the true frequency of *KRAS* mutations in brain AVMs.

In conclusion, we demonstrate that approximately one-third of brain AVMs harbor *KRAS* mutations that may be among key genetic drivers behind their development. *KRAS* p.G12 V was the most common *KRAS* mutation identified in our study. We also demonstrate the first reported instance of a *KRAS* p.G12C mutation in a brain AVM. The mean age of patients with *KRAS*-mutant AVMs was slightly lower than in the non-mutant group, and the mean size larger. In this study, all observed histologic criteria of brain AVMs were equally distributed and similarly present in all AVMs, regardless of *KRAS* status. This indicates that the clinical features and histology of brain AVMs are not specific to activating *KRAS* mutations and, therefore, that *KRAS* mutations in brain AVMS may be of little clinical or pathologic importance.

References

[1] Hetts SW, Cooke DL, Nelson J, et al. Influence of patient age on angioarchitecture of brain arteriovenous malformations. Am J Neuroradiol 2014;35:1376-80.

[2] Abecassis IJ, Xu DS, Batjer HH, et al. Natural history of brain arteriovenous malformations: a systematic review. Neurosurg Focus 2014;37:E7.

[3] Al-Shahi R, Warlow C. A systematic review of the frequency and prognosis of arteriovenous malformations of the brain in adults. Brain 2001;124:1900-26.

[4] van Beijnum J, van der Worp HB, Schippers HM, et al. Familial occurrence of brain arteriovenous malformations: a systematic review. J Neurol Neurosurg Psychiatry 2007;78:1213-7.

[5] Krings T, Kim H, Power S, et al. Neurovascular manifestations in hereditary hemorrhagic telangiectasia: imaging features and genotype-phenotype correlations. Am J Neuroradiol 2015;36:863-70.

[6] Eerola I, Boon LM, Mulliken JB, et al. Capillary malformation-arteriovenous malformation, a new clinical and genetic disorder caused by RASA1 mutations. Am J Hum Genet 2003;73:1240-9.

[7] Kim J, Kim OH, Suh JH, et al. Wyburn-Mason syndrome: an unusual presentation of bilateral orbital and unilateral brain arteriovenous malformations. Pediatr Radiol 1998;28:161.

[8] Nikolaev SI, Vetiska S, Bonilla X, et al. Somatic activating KRAS mutations in arteriovenous malformations of the brain. N Engl J Med 2018;378:250-61.

[9] Jinesh GG, Sambandam V, Vijayaraghavan S, et al. Molecular genetics and cellular events of K-Ras-driven tumorigenesis. Oncogene 2018;37:839-46.

[10] Haigis KM. KRAS alleles: the devil is in the detail. Trends Cancer 2017;3:686-97.

[11] Rauen KA. The RASopathies. Annu Rev Genomics Hum Genet 2013;14:355-69.

[12] Simanshu DK, Nissley DVMcCormick F. RAS proteins and their regulators in human disease. Cell 2017;170:17-33.

[13] Kleinschmidt-Demasters BK. Part II, section 3. Vascular diseases. In: Kleinschmidt-Demasters BK, Tihan T, Rodriguez F, editors. Diagnostic pathology: Neuropathology. 2nd ed. Philadelphia, PA: Elsevier; 2016. p. 762-7.

[14] Kalaria RN, Ferrer I, Love SP. Chapter 2. Vascular disease, hypoxia, and related conditions. In: Love SP, Budka H, Ironside JW, Perry A, editors. Greenfield's neuropathology. 9th ed. Boca Raton, FL: CRC Press, Taylor & Francis Group; 2015. p. 118-9.

[15] Porteous ME, Burn J, Proctor SJ. Hereditary haemorrhagic telangiectasia: a clinical analysis. J Med Genet 1992;29:527-30.

[16] Roman G, Fisher M, Perl DP, et al. Neurological manifestations of hereditary hemorrhagic telangiectasia (Rendu-Osler-weber disease): report of 2 cases and review of the literature. Ann Neurol 1978;4:130-44.

[17] Ayturk UM, Couto JA, Hann S, et al. Somatic activating mutations in GNAQ and GNA11 are associated with congenital hemangioma. Am J Hum Genet 2016;98:789-95.

[18] Couto JA, Huang L, Vivero MP, et al. Endothelial cells from capillary malformations are enriched for somatic GNAQ mutations. Plast Reconstr Surg 2016;137:77e-82e.

[19] Couto JA, Vivero MP, Kozakewich HP, et al. A somatic MAP3K3 mutation is associated with verrucous venous malformation. Am J Hum Genet 2015;96:480-6.

[20] Limaye N, Kangas J, Mendola A, et al. Somatic activating PIK3CA mutations cause venous malformation. Am J Hum Genet 2015;97:914-21.

[21] Limaye N, Wouters V, Uebelhoer M, et al. Somatic mutations in angiopoietin receptor gene TEK cause solitary and multiple sporadic venous malformations. Nat Genet 2009;41:118-24.

[22] Anglesio MS, Papadopoulos N, Ayhan A, et al. Cancer-associated mutations in endometriosis without cancer. N Engl J Med 2017;376:1835-48.

[23] Papke B, Der CJ. Drugging RAS: know the enemy. Science 2017;355:1158-63.

[24] Saeed O, Lopez-Beltran A, Fisher KW, et al. RAS genes in colorectal carcinoma: pathogenesis, testing guidelines and treatment implications. J Clin Pathol 2019;72:135-9.

[25] Patricelli MP, Janes MR, Li LS, et al. Selective inhibition of oncogenic KRAS output with small molecules targeting the inactive state. Cancer Discov 2016;6:316-9.

[26] Lito P, Solomon M, Li LS, et al. Allele-specific inhibitors inactivate mutant KRAS G12C by a trapping mechanism. Science 2016;351:604-8.

[27] Janes MR, Zhang J, Li LS, et al. Targeting KRAS mutant cancers with a covalent G12C-specific inhibitor. Cell 2018;172:578-89 [e517].
[28] Dang CV, Reddy EP, Shokat KM, et al. Drugging the 'undruggable' cancer targets. Nat Rev Cancer 2017;17:502-8.
[29] Einaga N, Yoshida A, Noda H, et al. Assessment of the quality of DNA from various formalin-fixed paraffin-embedded (FFPE) tissues and the use of this DNA for next-generation sequencing (NGS) with no artifactual mutation. PLoS One 2017;12:e0176280.